

- [15] Shi, A.-C., Desai, R.C. and Noolandi, J.  
*Phys. Rev. Lett.* (1997) 78, 2577.
- [16] Rosedale, J.H., Bates, F.S., Almdal, K. et al., *Macromolecules* (1995) 28, 1429.
- [17] Bates, F.S., Rosedale, J.H., Bair, H.E., et al., *Macromolecules* (1989) 22, 2557.
- [18] Hamley, I.W., Gehlsen, M.D., Khandpur, A.K. et al., *J. Phys. II*, France (1994) 4, 2161.
- [19] Hillmyer, M.A., Bates, F.S., Almdal, K. et al., *Science* (1996) 271, 976.
- [20] Rosedale, J.H., PhD Thesis, University of Minnesota (1993).
- [21] Fetters, L.J., Lohse, D.J., Richter, D. et al., *Macromolecules* (1994) 27, 4639.
- [22] Vigild, M.E., Almdal, K., Mortensen, K. et al., *Macromolecules* (1998) 31, 5702.

## Modelling diffraction patterns from a textured polycrystalline sample

Y. Nishiyama<sup>1</sup> and P. Langan<sup>2</sup>

1. Graduate School of Agricultural and Life Science,  
University of Tokyo, Yayoi, Tokyo 113-8657, Japan

2. B. Division, Los Alamos National Laboratory, MS-M888,  
Los Alamos NM87545 USA

## Introduction

Fibre diffraction studies have enabled structural information to be extracted from materials that are difficult to crystallize into macroscopic single crystals or when the state of interest is not highly crystalline. It is usually assumed that the sample is an aggregate of basic scattering units, each with an associated unique axis. The scattering units either exhibit rotational symmetry about the unique axis or the distribution of orientations about the unique axis is random. In addition to this, the distribution of the unique axis itself is given by a function that has rotational symmetry about a preferred direction, called the fibre axis. This is a good approximation for fibrous materials with diffraction information uniformly distributed around the fibre axis. However, there are fibrous, polycrystalline materials in which the distribution of the unique axis does not have rotational symmetry about the fibre axis or in which the scattering units are not uniformly orientated around the unique axis. The first effect is often referred to as texture. When the second effect corresponds to a second direction in the basic scattering unit being preferentially oriented around a second axis in the fibre it is referred to as biaxial orientation. In our studies of the crystal structure of native cellulose we have obtained sharp diffraction data extending to 1Å resolution (1) but exhibiting complex texture resulting from a combination of the two effects mentioned above. This problem also afflicts quasi-single-crystalline  $\alpha$ -chitin from which good data have been collected recently (2), but the refined structure has yet to emerge due to the lack of proper software to deal with diffraction data from a specimen of complex texture. This article describes a realistic approach to processing diffraction data from fibre specimens with complex texture and is illustrated with the structure of native cellulose as an example.

## The sample and diffraction data

The acquisition of diffraction data from highly oriented cellulose film specimens from the tunicate *Halocynthia roretzi* has been described elsewhere (3). The sample consisted of crystalline whiskers with polygonal cross-section which are about 20 nm in width and a few microns in length. A series of X-ray diffraction patterns was collected at 15° intervals around the main axis, and another series of patterns was obtained by tilting the main axis in 2° steps. Each frame was then converted to polar (RZ) coordinates on a 0.001 Å-spaced grid out to 1 Å without merging the four quadrants. Consequently each frame consisted of 2000 by 2000 pixels. The diffuse background was subtracted using the method by Sonneveld (4) extended into two-dimensions.

## Computation environment

The computation was carried out on a Linux system equipped with a Pentium III, 256 Mbytes of RAM,

and a gcc-2.95.2 compiler.

## Defining the texture

The texture of the sample can be determined experimentally by measuring the pole figures of two reflections that are in different directions (preferably perpendicular to each other). This can be readily measured when diffraction data are obtained through the whole of reciprocal space.

In the part which follows Cartesian coordinates (XYZ) are used to define principal directions in the sheet specimen (Y perpendicular to the plane, X and Z in plane).

## The orientation of the main axis:

Figure 1 shows the observed and fitted intensity distribution of the 004 reflection of the specimen. It can be seen that the unique axes of the crystallites have a broader distribution in a plane parallel to the film surface than perpendicular to it. The distribution function could be fitted with a two-dimensional Gaussian function of the form

$$I = \exp \left[ - \left( \frac{\mu}{b_1} \right)^2 - \left( \frac{v}{b_2} \right)^2 \right]$$

where  $\mu$  is the angle to the XZ-plane or the film surface,  $v$  is the angle to YZ-plane that is perpendicular to the film surface, and  $b_1$  and  $b_2$  are the standard deviations. In the present case  $b_1$  and  $b_2$  were 4.2° and 8.3° respectively. In a general case, the orientation distribution can be expressed as a function of  $(\mu, v)$ .

**The orientation of the second axis:** The existence of preferred orientation of the second axis can be seen in the diffraction pattern obtained with the beam parallel to the Z-axis (Fig. 2). The orientation of the second axis is confined to a circle around the main axis and can be described by only one parameter  $\omega$  which is defined here as the angle between the second axis  $e_2$  and the YZ plane. Thus an arbitrary orientation can be expressed by three parameters  $\mu, v, \omega$ , and a three-dimensional population density function  $\rho(\mu, v, \omega)$  can describe the texture of any polycrystalline sample.

## Calculation of azimuthal profile

A difference between  $b_1$  and  $b_2$  itself leads to an asymmetric diffraction pattern at a higher diffraction angle except when taken with the beam

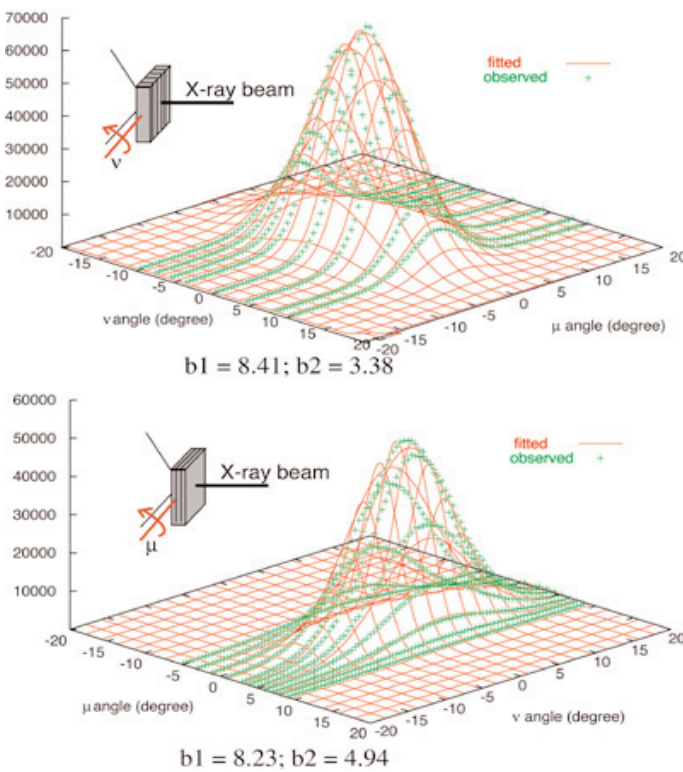


**Figure 1.** Observed and fitted azimuthal intensity profile of the 004 reflection. The fitted parameters were slightly different between the two sets of experiments and the mean value was taken to define the orientation of the c-axis.

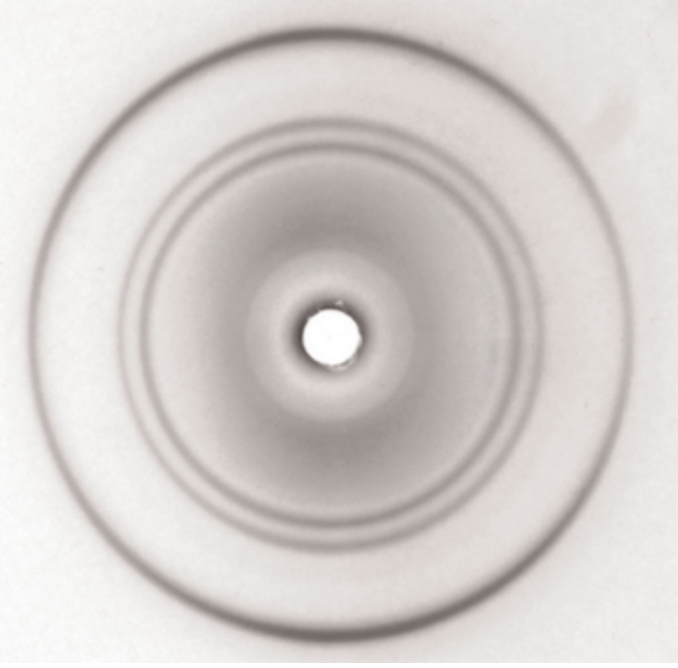


**Figure 2.** Diffraction diagram taken with the beam parallel to the main axis of the sample; the film surface is horizontal.

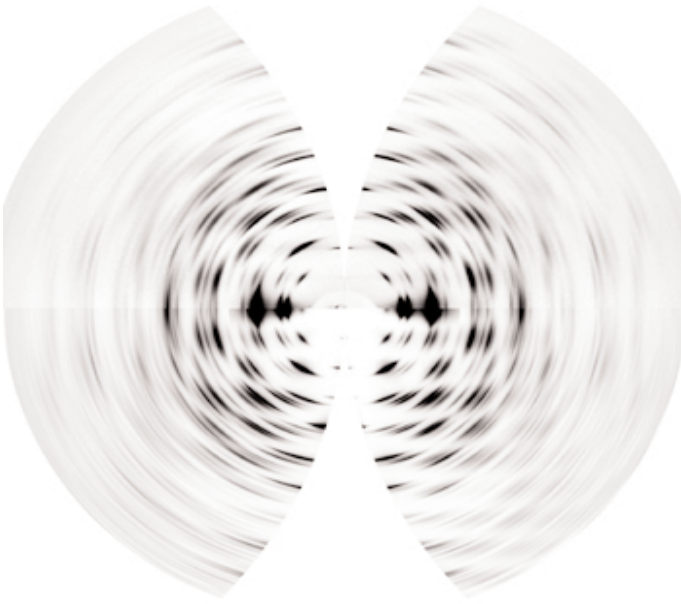


**Figure 3.** Asymmetric diffraction diagram from oriented cellulose film specimen. The upper half is observed data, and the bottom half is the simulated data.

perpendicular or parallel to the surface. An example is shown in Figure 3. Even if a symmetric diagram could be obtained, the azimuthal intensity profile of each reflection would not be the same as in the fibre case.

In the following analysis, the intensity calculation is for a reflection at position vector  $\mathbf{p}$  that makes an angle  $\sigma$  to the main crystallite axis  $\mathbf{e}_1$ , a dihedral

angle  $\phi$  around  $\mathbf{e}_1$ , and is at a distance  $r$  from the origin. Consider a position  $P$  that has a polar coordinate  $(r, \tau, \nu)$  as illustrated in Figure 4. The crystal contributing to the diffraction intensity at  $P$  due to the reflection  $\mathbf{p}$  has its main axis  $\mathbf{e}_1$  on a cone of semi-angle  $\sigma$  (i.e. between  $\mathbf{e}_1$  and  $OP$ ). The Cartesian coordinates of the orientation vector  $\mathbf{e}_1$  can be described using an angular parameter  $\theta$  as follows:

$$\mathbf{e}_1 = R(\nu)\mathbf{e}_1'$$

where:

$$\mathbf{e}_1' = \frac{r \tan \sigma \left[ \cos \theta \begin{pmatrix} 1 \\ 0 \\ 0 \end{pmatrix} + \sin \theta \begin{pmatrix} 0 \\ -\cos \tau \\ \sin \tau \end{pmatrix} \right] + P}{r / \cos \sigma}$$

$$= \begin{pmatrix} \sin \sigma \sin \theta \\ \cos \sigma \sin \tau - \sin \sigma \cos \theta \cos \tau \\ \cos \sigma \cos \tau + \sin \sigma \cos \theta \sin \tau \end{pmatrix}.$$

For a given orientation of  $\mathbf{e}_1$ , the orientation of  $\mathbf{e}_2$  is uniquely determined as

$$\mathbf{e}_2 = \frac{\mathbf{p} - (r \cos \sigma) \mathbf{e}_1'}{r \cos \sigma}$$

The number of crystals that are contributing to the intensity at that position can be calculated by integrating the population density function  $\rho$  over a circle on the cone, or

$$\begin{aligned} &= \int_{-\pi}^{\pi} \rho(\mathbf{e}_1, \mathbf{e}_2) \sqrt{\left(\frac{\partial \mu}{\partial \theta}\right)^2 + \left(\frac{\partial \nu}{\partial \theta}\right)^2} d\theta \\ &= \int_{-\pi}^{\pi} \rho(\mathbf{e}_1, \mathbf{e}_2) \sqrt{\cos^2 \theta + \sin^2 \theta \cos^2 \tau} d\theta \end{aligned}$$

The integration cannot be obtained analytically for most types of function  $\rho$  and should be obtained numerically. The integration for grid points of appropriate interval and range in reciprocal space can be

$$I(P) = \int_C \rho(P) = \int_{-\pi}^{\pi} \rho(\mathbf{e}_1, \mathbf{e}_2) \left| \frac{\partial \mathbf{e}_1}{\partial \theta} \right| d\theta$$

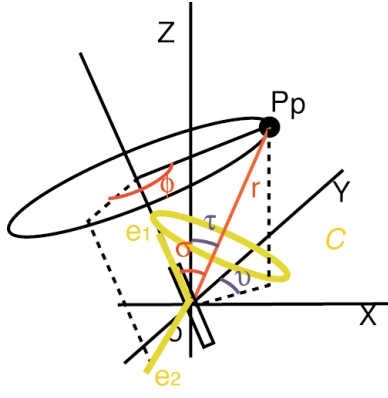


**Figure 4.** Schematic illustration to define the geometry parameters.

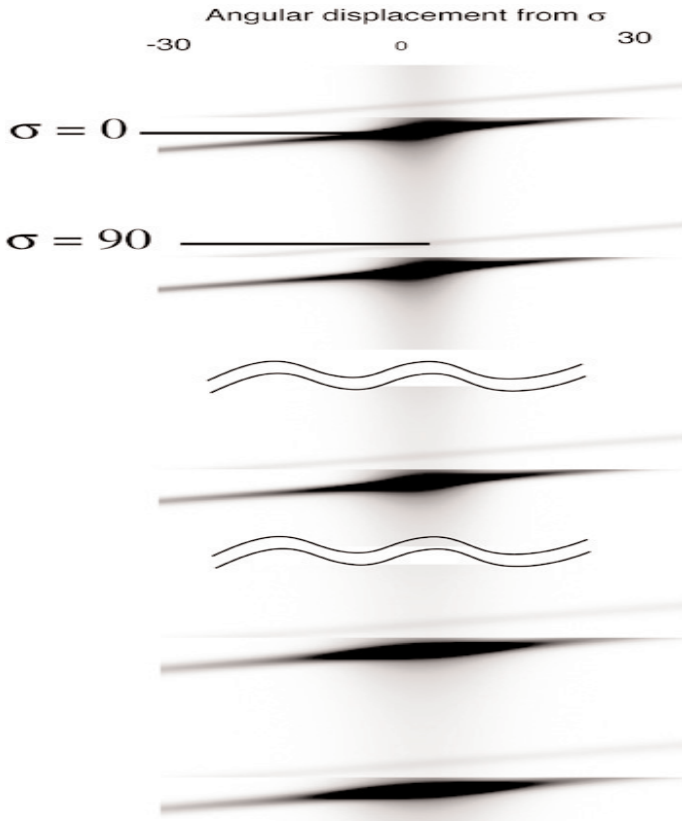


**Figure 5.** Part of the grid data representing the azimuthal intensity distribution shown in grey scale.

calculated and stored to be interpolated on use. Note that the integration is independent of  $r$  and only depends on  $\sigma$ ,  $\tau$ ,  $\nu$  and  $\phi$ . Thus the azimuthal intensity profile should be stored in a 4-dimensional array in the most general case. If the texture is such that the orientation of  $\mathbf{e}_2$  is independent of the orientation of  $\mathbf{e}_1$ , or

$$\rho(\mu, \nu, \omega) = \rho_1(\mu, \nu)\rho_2(\omega),$$

and  $\rho_1$  is much sharper than  $\rho_2(\omega)$ , then  $I(P)$  can be approximated as:

$$I(P) \approx I_2 \cdot I_1 = \rho_2(\nu - \phi) \int_{-\pi}^{\pi} \rho_1(e_1) d\theta$$

and the profile can be stored in two arrays, one of 3-dimensions and one of 1-dimension, to economise on memory and CPU time. This was done in the case of the cellulose sample.

The DQAGE routine from the Fortran mathematical library QUADPACK [5] used to calculate the integration and the interpolation routine for even spaced multi-dimensional grids was obtained from Magic Software Inc. [6]. The evaluation of  $I_1$  in  $200 * 100 * 30$  grid points took about 5 min. Figure 5 shows the array as a grey image.

### Determination of the orientation of the second axis

Since the volume of specimen in the beam varied when the specimen was rotated around the Z-axis, the orientation of the second axis was evaluated by comparing the intensity of three reflections on the equator. It would be possible to arrange experiments so as to ensure that there is a constant specimen volume in the beam path, for example by using smaller samples, but this leads to a higher background which is not desirable. Thus the orientation of the second axis was determined from the relative intensities of several clearly resolvable reflections. The intensity ratios of the three most intense reflections,  $I_{200}$ ,  $I_{110}$  and  $I_{1-10}$  of the cellulose I data are plotted in Figure 6.

Since there should be equal numbers of up and down crystals, and if the  $\mathbf{a}$ -axis is taken as  $\mathbf{e}_1$ , then:

$$I_{rel} = \frac{I_1(\omega)}{I_2(\omega)} = I_{12} \frac{\rho_2(\omega - \phi_1) + \rho_2(\omega + \phi_1)}{\rho_2(\omega - \phi_2) + \rho_2(\omega + \phi_1)}$$

In a matrix expression for a discrete set of  $\rho_2$ :

$$\rho_2(\omega - \phi_1) = \Phi_1 \rho_2(\omega)$$

$$\Phi_1 = \begin{pmatrix} \phi_1 & n-\phi_1 \\ \bullet & \bullet \\ \bullet & \bullet \\ \bullet & \bullet \\ \bullet & \bullet \end{pmatrix}$$

$$(\Phi_1 \rho_2 + \Phi_{-1} \rho_2) \cdot \mathbf{I}_{rel} = (\Phi_2 + \Phi_{-2}) I_{12} \rho_2 ,$$

$$((\Phi_1 + \Phi_{-1}) \mathbf{I}_{rel} - (\Phi_2 + \Phi_{-2}) I_{12}) \rho_2 = 0$$

thus  $I_{12}$  can be obtained by solving:

$$|(\Phi_1 + \Phi_{-1}) \mathbf{I}_{rel} - (\Phi_2 + \Phi_{-2}) I_{12}| = 0$$

$\rho_2$  can be obtained as an eigenvector. When using several combinations of reflections, a least squares solution can be obtained by solving the following matrix equation with standard matrix inversion:

$$\begin{pmatrix} \mathbf{A}_1 \\ \mathbf{A}_2 \\ 1 & L & 1 \end{pmatrix} \rho = \begin{pmatrix} O \\ O \\ 1 \end{pmatrix}$$

where

$$\mathbf{A}_i = (\Phi_i + \Phi_{-i}) \mathbf{I}_{rel} - (\Phi_j + \Phi_{-j}) I_i$$

The resulting orientation function  $\rho$  and the density profiles of the 200 and 110 reflections are plotted in Figure 7. The reflection profiles become symmetric due to the presence of up and down crystals.

### Calculation of the radial profile

Radial broadening comes solely from instrumental broadening, finite crystal size and the presence of crystal imperfections, and can be treated independently of the orientation issue. To analyse this, we used a pseudo-Voigt function of the form:

$$f = \frac{A}{C} \{D * G + (1 - D) * L\}$$

$$G = 2\sqrt{\frac{\ln 2}{\pi}} D \exp\left\{-4 \ln 2 \left(\frac{x - B}{C}\right)^2\right\}$$

$$L = \frac{4}{\pi \left\{1 + 4 \left(\frac{x - B}{C}\right)^2\right\}}$$

where  $A$  is the peak area,  $B$  is the peak position,  $C$  is the full width at half maximum (FWHM) and  $D$  is a shape parameter between 0 and 1.

### Construction of the normal equation

Usually the observed intensities are due to multiple reflections, and modelling is done for the purpose of resolving each component as far as possible. If the

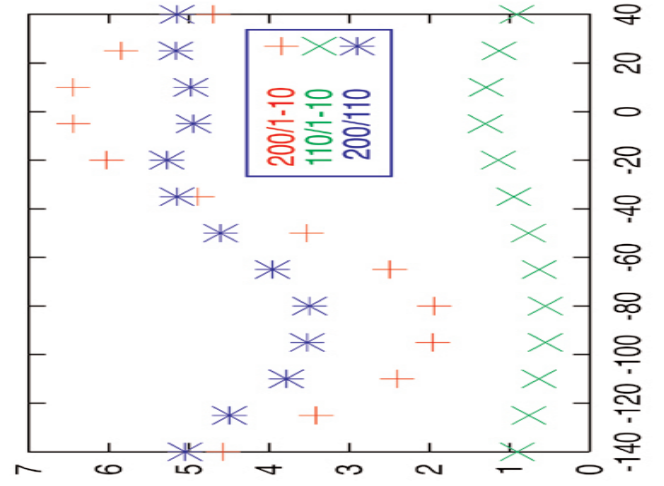


**Figure 6.** Plot of intensity ratios among the three strongest equatorial reflections from the cellulose sample taken at different rotations around the main axis.

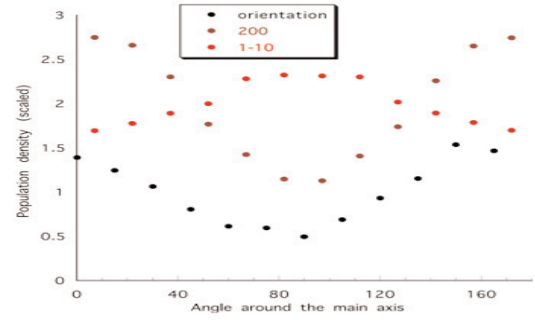


**Figure 7.** The orientation function and the simulated reflection intensity profile around the main axis. The intensity profiles are symmetric and up and down crystals are assumed to contribute equally.

orientation distribution and the radial profile are known, the least-squares fitting to the observed data  $\mathbf{y}_{obs}$  is a linear problem:

where  $\mathbf{a}_i$  is the profile of the  $i$ th reflection. If the number of data values is  $m$ , then  $\mathbf{A}$  is a matrix of size  $n$  by  $m$ . This can be directly solved if  $m$  is not too big. With an oriented sample,  $\mathbf{A}$  is a sparse matrix as each reflection contributes to only a small number of data. Although  $\mathbf{A}$  is sparse and could be stored in more compact form, the observed data extend throughout 3-dimensional reciprocal space and would be too numerous. A normal equation is thus constructed as:

$$\tilde{\mathbf{A}}\mathbf{A}\mathbf{f} \equiv \mathbf{B}\mathbf{f} = \mathbf{A}\mathbf{y}_{obs} \equiv \mathbf{b}$$

$$\text{or, } B_{kl} = \sum_{j=1}^n \sum_{i=1}^n A_{ki} A_{jl}$$

The direct calculation of  $B$  needs  $n$ -by- $n$  function evaluations for each of the  $m$ -by- $m$  elements. However, since only a limited number of reflections can contribute to a given position, the potentially-contributing reflections were chosen prior to each

$$\mathbf{y}_{obs} = \mathbf{a}_1 * f_1 + \mathbf{a}_2 * f_2 \dots \mathbf{a}_n * f_n = \mathbf{A}\mathbf{f}$$

calculation of element  $B_{kl}$ , and the summation was carried out only within a subgroup of  $(i, j)$  to make the calculation feasible. In the present case, the reflections within a radial limit of  $0.03 \text{ \AA}^{-1}$  and within  $30^\circ$  in an azimuthal direction were included.

### Singularity issues

The above matrix  $B$  is singular if there are reflections that are very close compared to the sharpness of the peak, which is the case for most polycrystalline samples. This means that the normal equation cannot be solved by usual matrix inversion; actually there is no way to know the individual intensity. Consequently the singular value decomposition (SVD) method was chosen as a way to easily filter degenerate components. The DGELSD, a LAPACK [8] driver routine, was used to calculate the minimum norm least-squares solution. The routine gives back the effective rank of the normal matrix  $B$ .

The calculation of 12 frames together, including about 800 reflections, took about 80 hours of computation time to construct and to solve the normal equation. The effective rank was 625. The simulated image of half of a frame is shown in the lower part of Figure 3.

### The Lorenz-Polarization factor

Since the calculated azimuthal profiles are already based on the number of reflections contributing to the observed intensity, no consideration is needed for the factor due to orientation. The only correction needed to obtain the structure factor is the distance of the reflection from the centre in reciprocal space, as the density diminishes by the square of the distance.

### Conclusion

The azimuthal profile of any reflection from a polycrystalline specimen can be calculated by numerical integration of a function defining the texture. A series of diffraction patterns could be simulated in an acceptable time using a standard computational environment.

### Acknowledgements

We thank Dr. H. Chanzy for valuable suggestions for the conduct of the work.

### References

- [1] Presented at the CCP13 Workshop 2000.
- [2] H. Chanzy, *Advances in Chitin Science*: Jacques Andre Publishers, France (1998) Vol.II, 11-21.
- [3] Y. Nishiyama, S. Kuga, M. Wada, T. Okano, *Macromolecules* (1997) 30, 6395.
- [4] E. J. Sonneveld & J. W. Visser, *J. Appl. Cryst* (1975) 8, 1.
- [5] <http://www.netlib.org/quadpack/>
- [6] <http://www.magic-software.com/>
- [7] <http://www.netlib.org/lapack/>